Astronomy & Astrophysics manuscript no. aa˙osc2 August 6, 2003
(DOI: will be inserted by hand later)

Observations of oscillations in the transition region above sunspots

J. Rendtel[1], J. Staude[1] and W. Curdt[2]

[1] Astrophysical Institute Potsdam (AIP), Sonnenobservatorium Einsteinturm, Telegrafenberg, 14473 Potsdam, Germany
e-mail: `jrendtel@aip.de`

[2] Max-Planck-Institut für Aeronomie, 37191 Katlenburg-Lindau, Germany
e-mail: `curdt@linmpi.mpg.de`

Received 5 June 2003 / Accepted 29 July 2003 / Version received 15 July 2003

Abstract. Observations during two campaigns of the SUMER spectrograph and the EIT imager onboard SoHO were used to analyse oscillations in bright sunspot plumes. We report variations of both intensity and velocity seen in EUV emission lines originating in the sunspot upper chromosphere and the transition region. The wavelet analysis reveals rapidly changing conditions in the emitting volumes. Generally, oscillations in the 5 min range dominate in the chromosphere, while the transition region lines show oscillations at shorter periods (2 to 3 min). A drift of the oscillation period of the Doppler velocity from 5 min to 2.5 min within about 30 minutes can be explained by a strongly non-stationary behaviour of the upper chromosphere and transition region, probably related to downstream of material within the plume region. Synchronous EIT observations of the lower corona show no intensity oscillations. This hints either at a strong damping or a downward reflection in the upper transition region or lower corona.

Key words. Sun: chromosphere – Sun: transition region – Sun: oscillations – sunspots

1. Introduction

Observations of UV spectral lines formed in the chromosphere-corona transition region (CCTR) above sunspots with the UVSP instrument aboard the SMM spacecraft led to the discovery of significant oscillations of velocity, δv, and occasionally of intensity, δI (Gurman et al. 1982; Henze et al. 1984; Thomas et al. 1984). Sharp resonance peaks of the power of δv and δI, particularly observed in the umbra, show a characteristic height dependence of frequencies and phases. Peaks in the 2…3 min period band appear as a continuation of chromospheric umbral oscillations.

Such a behaviour can be explained by the resonant transmission of magneto-atmospheric waves through the sunspot atmosphere. Models of coupled resonators (Žugžda et al. 1983, 1984, 1987; Settele et al. 1999) require regions of strong wave reflection, e.g. from the steep temperature gradient of the CCTR. Consequently, oscillations should be observed in EUV lines in the sunspot CCTR as well. Theoretical modelling of intensity oscillations in optically thin EUV lines requires velocity oscillations without intensity fluctuations in the adiabatic case. On the other hand, measurements of intensity oscillations would hint at a non-adiabatic behaviour such as that of almost isothermal waves (Žugžda et al. 1984; Staude et al. 1985). Such a result is important because inferences of propagating waves (e.g. Brynildsen et al. 1999a, 1999b) are often obtained explaining the data by a theory of adiabatic sound waves. Reviews on both observations and interpretations of sunspot oscillations have been given by Staude (1999) and Bogdan (2000). Recent observations using data from various instruments contribute to the understanding of the processes in the CCTR.

The present investigation aims at a deeper insight into the oscillatory processes, having available more complete data, that is, longer time series and simultaneous measurements in several CCTR and lower corona lines, including those corresponding to higher temperatures.

2. Observations and Data Reduction

Long time series of intensity and Doppler velocity data have been derived from two observing runs of the SUMER spectrograph aboard the SoHO spacecraft. The basic data of the observations are listed in Tab. 1.

Send offprint requests to: J. Rendtel

We refer to the observations taken on 1996 August 29 as data set A and to the observations on 1999 October 29 as data set B, respectively.

During the first campaign, A, the SUMER scanning mode was available. Scans of a sunspot consisting of six spectra, with raster steps of 1.14″ were made for 4.4 hours. This allows to compare a raster image of the scanned plume region above the sunspot in the light of the selected EUV lines with other images obtained e.g. with the EIT telescope (Fig. 1). EIT images were taken simultaneously to the first two hours of the SUMER observations (see Tab. 1). The inherent disadvantage of raster scans is the limited temporal resolution of the data concerning the plume position above the umbra as only every sixth spectrum refers to this position. There are no further SoHO data available for any time close to our campaign.

An extrapolation of the force-free magnetic field of the region NOAA 7986 (Fig. 2) was calculated based on the Kitt Peak magnetogram of 1996 August 29. These data provide important information concerning the structure of the region and for the interpretation of the observations (see Sect. 4).

The second observation, B, with the SUMER spectrograph was done at a fixed slit position with the solar rotation compensation switched on. The higher cadence of spectra gives a better temporal resolution allowing to search for higher frequency oscillations. We chose the MDI magnetogram obtained at 16:00 UT for an extrapolation of the force-free magnetic field of the region NOAA 7986 (Fig. 3). Most field lines connect to the spot of opposite polarity east of the major spot. The field lines extend essentially vertical from the main spot indicating that the oscillations should follow a vertical path from the photosphere through the CCTR to the lower corona. Hence we can assume that identical x, y-positions concern a common oscillating flux tube.

Targets of both series were sunspots with a bright EUV plume (Brynildsen et al. 2001). In the region *NOAA 7986* we observe variations in intensity δI and velocity δv in the transition region lines Ne VIII at 770.4 Å in second order and C IV at 1548.1 Å. Further, we analyse EIT intensity data in the corona lines of Fe IX/X at 171 Å. Information about the chosen spectral lines is summarized in Tab. 2.

The Lyman lines observed in *NOAA 8742* originate from the chromosphere. Additionally, the transition region line N III at 992.3 Å appearing in the same spectral region provides information about oscillations at larger heights (see Tab. 2 and Wilhelm et al. 1995).

Extrapolations of the magnetic field lines in both regions support the assumption that the bright EUV plume regions are situated vertically above the major sunspot of the two regions. Details of possible effects of deviations from a vertical direction are discussed later.

In order to improve the signal-to-noise ratio, we integrated over 3×3 pixels in the Ne VIII and C IV lines, and over 5×5 pixels in the Lyman and N III lines. Because we know that structures in the chromosphere and the transition region extend over areas larger than the intergrated pixels, this does not affect our results. Further, it has been shown that oscillations occur coherently over larger regions as well (Brynildsen et al. 1999a, 1999b). Both sunspots were localized within less than 20° from the solar disk centre so that geometrical effects are neglible.

Table 1. SUMER observations of large sunspots and supporting measurements of other SoHO and ground based instruments.

Set A: 1996 August 29, NOAA 7986		
SUMER:		
pointing	$x = -92.7'' \pm 5.0'', y = -296.3''$	
detector A		
slit $1'' \times 120''$		
C IV	1548.1 Å	09:08–13:31 UT
Ne VIII	770.4 Å	09:08–13:31 UT
temporal resolution 65.2 s		
EIT:		
Fe IX / X	171 Å	09:00–10:59 UT
temporal resolution 36 s		
Kitt Peak Obs.:		
magnetogram		16:34–17:29 UT
Set B: 1999 October 29, NOAA 8742		
SUMER:		
pointing	$x = -21.3'' \ldots 11.6'', y = 39.0''$	
detector A		
slit $0.3'' \times 120''$		
Lyman lines near	926 Å	13:20–15:04 UT
among these:		
H I Lyman 5	937.8 Å	13:20–15:04 UT
H I Lyman 9	921.0 Å	13:20–15:04 UT
H I Lyman 15	915.3 Å	13:20–15:04 UT
Ly continuum	907 Å	13:20–15:04 UT
lines near	1020 Å	15:05–16:48 UT
among these:		
H I Lyman β	1026.0 Å	15:05–16:48 UT
N III	992.3 Å	15:05–16:48 UT
temporal resolution 28.1 s		
MDI:		
magnetogram		16:00 UT

Both data sets were decompressed, flat-fielded and corrected for geometrical distortion effects applying standard software routines of the SUMER-soft library.

3. Wavelet analysis and oscillations

Both data sets are characterized by rapid changes of the intensity and Doppler velocity, respectively. Investigations of such non-stationary processes require methods which allow to localize various oscillations existing for typical periods of 10 to 20 minutes in time. For this purpose we applied a wavelet analysis to our data. Investigations of artificial data series show that small variations in frequency

Table 2. Spectral lines used for the analysis of intensity and Doppler velocity data. Data for the Lyman lines from Curdt & Heinzel (1998).

Line	λ	T_{eff}	Region
Fe IX/X	171 Å	$1.3 \cdot 10^6$K	lower corona
Ne VIII	770.4 Å	$6 \cdot 10^5$K	upper CCTR
C IV	1548.2 Å	$1 \cdot 10^5$K	lower CCTR
N III	992.3 Å	$8 \cdot 10^4$K	lower CCTR
H I Ly β	1026.0 Å	$2.8 \cdot 10^4$K	chromosphere
H I Ly 5	937.8 Å	$2.4 \cdot 10^4$K	chromosphere
H I Ly 9	920.9 Å	$1.23 \cdot 10^4$K	chromosphere
H I Ly 15	915.3 Å	$8.97 \cdot 10^3$K	chromosphere

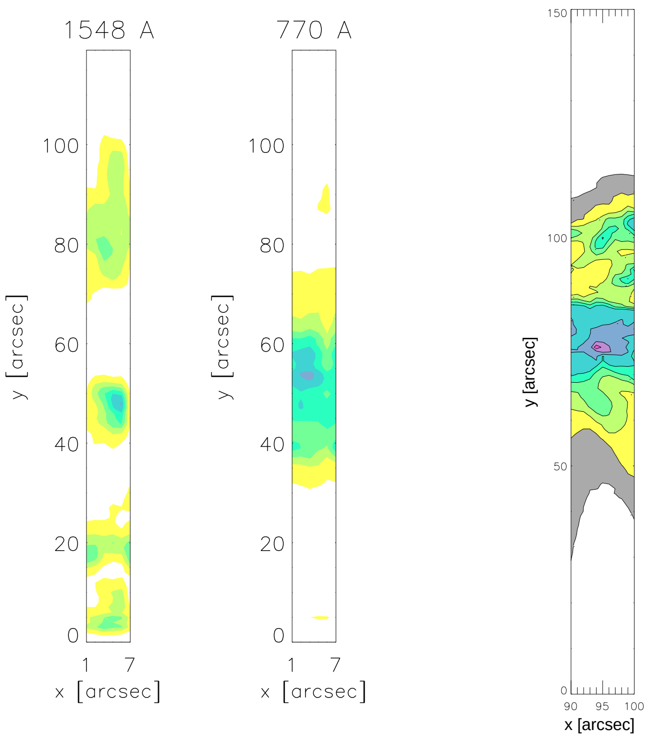

Fig. 1. Images of the EUV intensity reconstructed from SUMER scans of set A in the lines C IV 1548.1 Å (left; transition region) and Ne VIII 770.4 Å (centre; upper transition region) above the active region NOAA 7986 using 8 scans between 10:50 and 11:00 UT. The bright EUV structure is close to the centre. The strip on the right shows the respective band from the EIT filtergram in the lines of Fe IX/X 171 Å at 10:55 UT.
The sunspot is located close to the centre of the strips and has a diameter of about 10″ (cf. also Fig. 2). The intensity scale is inverted – dark patches represent high EUV intensity.

as well as short appearances (about 10 min) of oscillations even close (approximately 0.3 mHz) to dominating frequencies can be reliably detected (Rendtel 2001). Due to the finite length of the time series, it is not possible to analyse oscillations close to the start and end of the measurements. The width of the edge effect (cone of influence, Torrence & Compo 1998) depends on the length

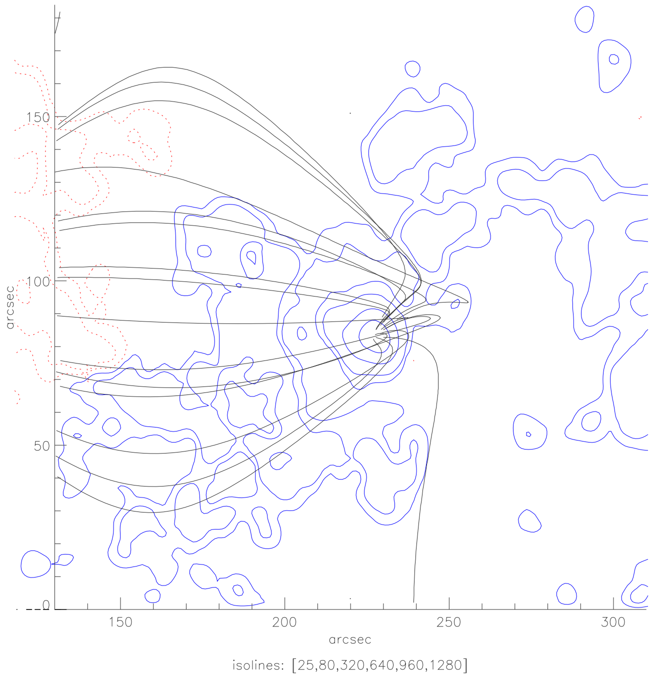

Fig. 2. Extrapolated magnetic field of the region NOAA 7986 on 1996 August 29 projected on the solar surface. We only show those field lines connecting the major spot with the region of opposite polarity. The spot is located within a large area of negative (south) polarity with a depletion to the NE (N is up, E is left).

of the time series and the frequency. In our case we find an extension of the cone of influence of 6 min at 7 mHz, and 10 min at 3 mHz, respectively. A minimum significance level of 0.8 was chosen for all oscillations shown and listed (Tab. 3) in this paper.

The results are shown in a number of graphs (Figs. 4 to 7) which consist of three panels each. The major (upper left) part shows the variation of oscillatory power for δI and δv, respectively, with the maximum power inside this diagram set to 100. The right panel shows the integrated power over frequency, and in the lower panel the temporal variation of the power at the indicated frequency(ies) is plotted.

Intensity and velocity oscillations in the frequency range 3…7 mHz as shown in Fig. 4 occur in all investigated spectral lines. This investigation is based on measurements of the line centre. Recently, Brynildsen et al. (2003) used measurements in the opposite wings of optically thin emission lines for analyses of oscillations above sunspots. Their results are similar to our findings as we will describe later. Generally, the typical duration of clearly visible oscillations in the CCTR and lower corona is of the order of 10 to 20 minutes, occasionally up to 40 minutes.

We also applied a wavelet analysis to the EIT intensity data in the coronal Fe IX/X lines obtained simultaneously with the Ne VIII and C IV lines in the region NOAA 7986 (cf. Tab. 1). Surprisingly, this analysis does not reveal any

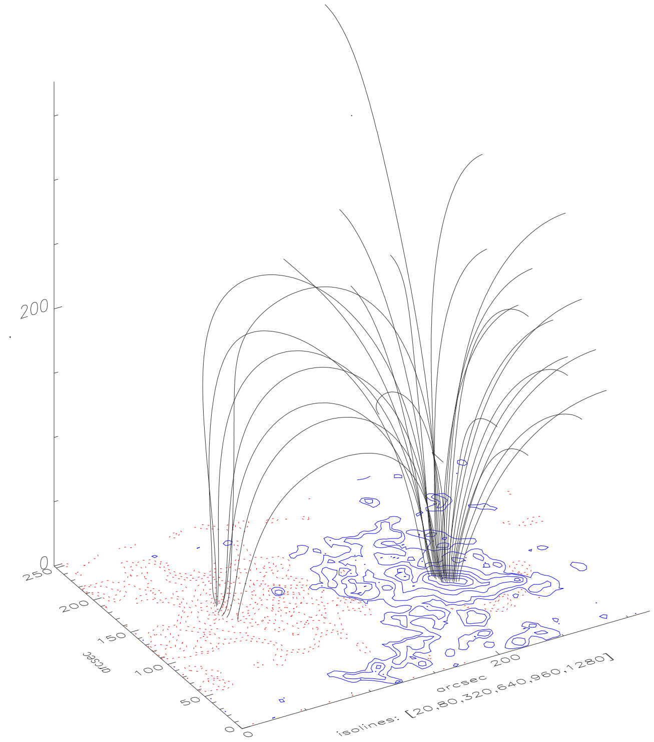

Fig. 3. Perspective view on the extrapolated magnetic field of the region NOAA 8742 on 1999 October 29 based on the MDI magnetogram obtained at 16:00 UT. The major spot is located in the large area of negative (south) polarity (N is up, E is left). Field lines starting from the spot area in the photosphere are almost vertical up to a few 10^4 km. The vertical z-axis gives the altitude above the photosphere in arcsec ($1'' \approx 700$ km).

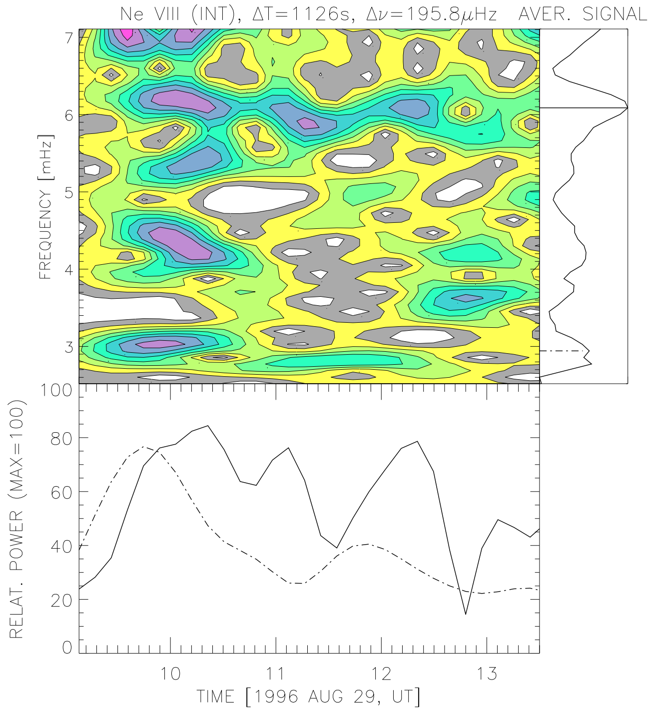

Fig. 4. Intensity oscillations in the Ne VIII line in the plume above the spot in NOAA 7986 (set A). Most of the time we find a 6.2 mHz oscillation while the 5 min oscillation (near 3 mHz) appears only in the first hour (dashed line).

intensity oscillation in the frequency range between 3 and 7 mHz, although we made every effort to correct for possible trends or to filter smaller frequencies (Rendtel 2001).

Generally, the oscillations of Doppler velocity (line-of-sight velocity) and the intensity occur in the same frequency ranges. At three occasions we found a drift of the frequency of the Doppler velocity towards higher frequencies with a drift rate of about 3 mHz/h. This concerns the Ne VIII line (Fig. 5), where we first find a peak of oscillatory power at 4 mHz (dashed line) followed by a peak at 6 mHz (solid line) about 40 minutes later. Another such drift is found in the transition region line N III (Fig. 6) from 4 mHz to 6.5 mHz within about 30 minutes. This is followed by a similar and virtually simultaneous drift in the chromospheric Lyman β line from 3 mHz to about 5 mHz (Fig. 7).

4. Interpretation of the results

If we assume the resonant transmission of magneto-acoustic gravitational (MAG) waves being the source for the observed oscillations, we have to conclude that the resonance conditions obviously vary rapidly within short periods of time. Typical time scales are of the order of 10 to 30 minutes. Hence we often will observe about ten periods until the oscillation decays or becomes too small to be detected.

Resonant transmission and filtering of MAG waves was shown to allow selected frequencies to reach coronal heights (Žugžda et al. 1987, Settele et al. 1999, 2001). Numerical simulations for realistic values of the adiabatic coefficient γ and turbulent pressure $p_{\rm tu}$ published by Staude et al. (2001) show that particularly oscillations near 3…3.5 min (5.5…4.5 mHz) are expected to have a large transmission coefficient.

The observed drift of oscillations in the chromosphere (Lyman β) as well as in the CCTR towards higher frequencies at three occasions (cf. summary of results in Tab. 3) may be explained with a shrinking resonator size. Oscillations propagating downwards parallel to magnetic field lines reach regions of considerably converging flux tubes. Furthermore, the observability and the line-of-sight component of the Doppler velocity depend on the direction of the magnetic field. The extrapolated field of the region NOAA 7986 indicates that an oscillating volume may change its direction relative to the line of sight while moving along the field lines and thus cause a variation of the observed velocity and its variation (Fig. 8).

The CCTR lines Ne VIII, C IV and N III are optically thin lines. As already pointed out, the existence of oscillations in intensity δI hints at deviations from adiabatic conditions, possibly almost isothermal waves. The lack of intensity oscillations in the corona as derived from the EIT measurements may be explained by different effects. Possible reasons are a strong damping or a dominating

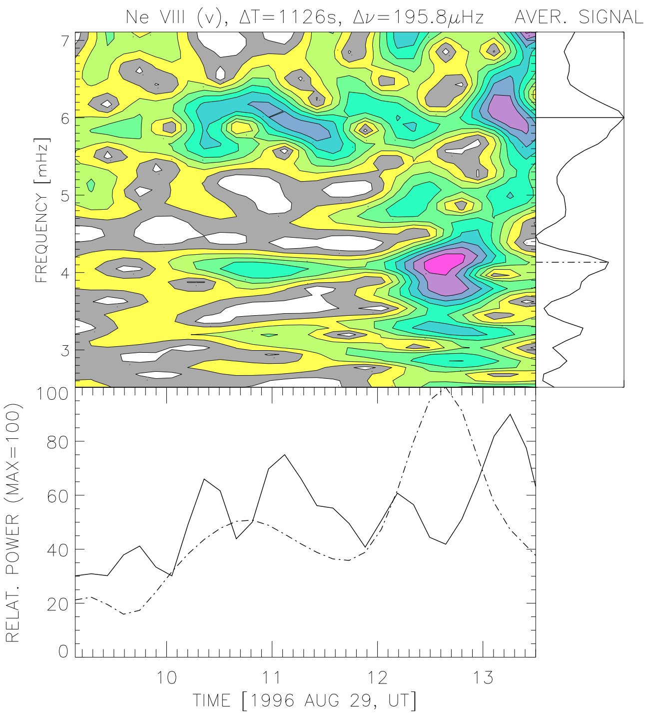

Fig. 5. Velocity oscillations in the Ne VIII line (NOAA 7986, set A). The most prominent frequency is near 6 mHz (solid line), but the oscillations show rapid temporal changes.

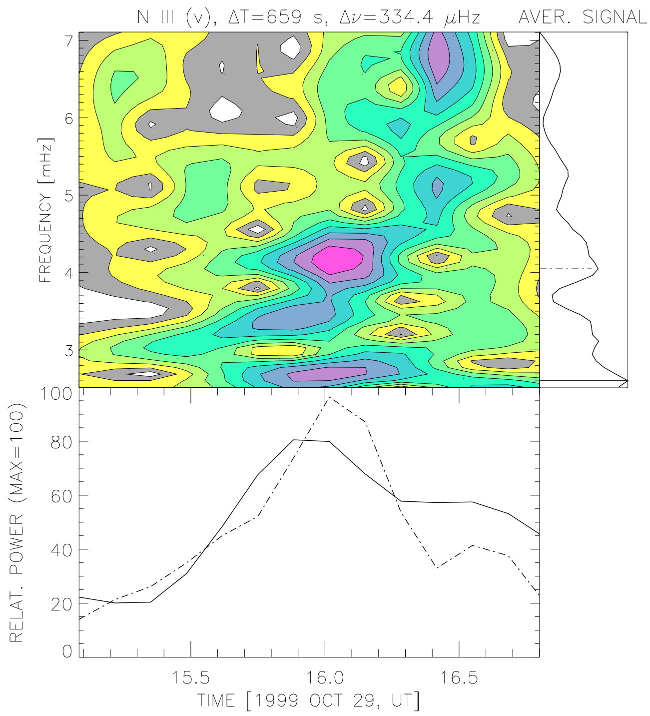

Fig. 6. Velocity oscillations in the N III line in the plume above the spot in NOAA 8742 (set B). A peak at 4 mHz is followed by oscillatory power at higher frequencies in the subsequent time.

downward reflection of the waves below the 10^6 K level. It is also possible that adiabatic conditions exist up to the CCTR, but not further towards the corona. However, one has to bear in mind that the observed rapid variations of the occurrence of various oscillations can be caused by temporary and/or spatially changing conditions. This is consistent with results described by Maltby et al. (1999), Brynildsen et al. (2002) and DeMoortel et al. (2002).

Phase relations between the intensity and velocity data persisting for a substantial portion of the time series are not detectable in our data of August 29, 1996, covering a large height range. If the conditions were adiabatic, a phase shift of 0° would hint at running waves, while a phase shift of 90° indicated standing waves. Perhaps the phase relations are rapidly changing if larger height scales are considered. The analysis of the chromospheric Lyman lines covering a height range of roughly 400 km (Curdt & Heinzel 1998) yields a phase velocity during our observation period of about 7 km/s which is close to the velocity of sound in the region of the line emission. However, even over this small range the phase relations between the oscillations are far from constant for more than about 20 minutes (Rendtel 2001). Curdt & Heinzel (1998) derived a phase velocity of about 3 km/s in the network outside sunspots.

The CCTR is a highly variable region which is not fixed in its vertical position and range. In bright EUV plumes we see a rather extended "cool" region, while other regions in close vicinity may be characterized by hot material moving down to geometrically low heights causing a transition region which has a small vertical extension only. From the existence of a variety of emission lines of 5 to 8-fold ionized species which are not found anywhere else on the Sun Curdt et al. (2000) concluded that the CCTR must have an entirely different height profile than the normal solar atmosphere and is probably much more extended in the quasi-open magnetic field lines. In this context we may assume that the existence of plumes strongly improves the visibility of oscillations as the emission of optically thin EUV lines is more effective. This is obvious from several other observations of oscillations in the CCTR (Fludra 1999, 2001; Ireland et al. 1999; O'Shea et al. 2001).

Rapid changes of the conditions are obviously typical for the CCTR. This is also underlined by observations of phenomena such as blinkers and explosive events. Blinkers are found to occur on time scales of 400 to 1600 s and are observed above sunspots as well (Harrison et al. 1999, Brković et al. 2000).

Radio observations at 17 GHz using the Nobeyama radio heliograph (Gelfreikh et al. 1999, Shibasaki 2001) show oscillations of radio brightness above sunspots near 6 mHz for periods of about an hour. Shibasaki related these oscillations with sound waves from lower levels in the solar atmosphere moving upwards and becoming visible as third harmonic at 17 GHz. The frequency near 6 mHz obviously appears during the entire data series. However, the analyses do not show temporal variations in the oscillation power. This observation concerns a geometrically rather low, hot and vertically thin CCTR. Conditions may be less variable than in the plume areas which we observe

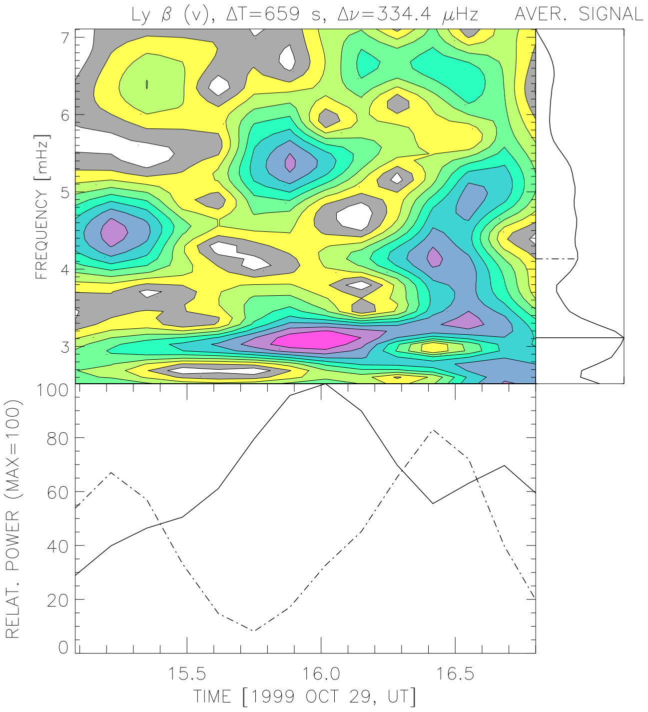

Fig. 7. Velocity oscillations in the chromospheric Lyman β line (NOAA 8742, set B). Most of the time we find a frequency near 3 mHz (5 min oscillation). Simultaneously to the drift in N III, we also see oscillatory power at higher frequencies.

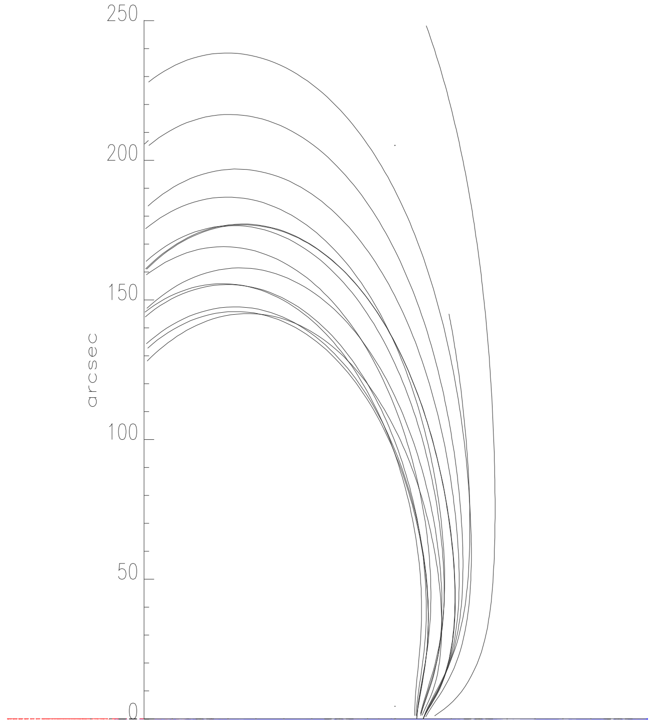

Fig. 8. View at the extrapolated field lines of Fig. 2 (NOAA 7986) from the south. Starting from the spot, the field lines are first directed somewhat in westerly direction before they turn to the east at larger heights. (1″ refers to about 700 km.)

Table 3. Power maxima of the oscillations found in the different lines from our wavelet analyses. t stands for temporarily occurring oscillations, l denotes oscillations observable at specific locations only. An arrow ($\rightarrow$) refers to a drift of the frequency as described in the text.

line	Intensity osc.	Velocity osc.
Set A: 1996 August 29, 09:08–13:31		
Ne VIII	6 mHz, 3 mHz *(t)* 7.3 mHz *(t)*	6 mHz, 4→6 mHz
C IV	6 mHz; 3 mHz 7.3 mHz *(t)*	3 mHz; 6 mHz *(t)*
Fe IX/X	none found	—
Set B: 1999 October 29, 13:20–15:04		
Ly 5	3.5 mHz *(t)* 7.2 mHz *(t)*	3.3 mHz 7 mHz, 5 mHz *(t)*
Ly 9 Ly 15 Ly cont.	7 mHz; 3.5 mHz 7 mHz; 3.5 mHz 7 mHz; 3.5 mHz	
Set B: 1999 October 29, 15:05–16:48		
Ly β	7 mHz; 3.5 mHz	3.2 mHz 3.3→4.5 mHz
N III	3.5 mHz; 5 mHz *(t)* up to 7 mHz *(l)*	3→7 mHz 3 mHz; 3.5 mHz *(l)*

when using the EUV emission lines. Hildebrandt & Staude (2002) found from model calculations that magnetic field variations of ±35 G as well as density and temperature fluctuations due to an oscillation of the CCTR in height with an amplitude of approximately 50 km could produce the measured microwave oscillations.

According to Brynildsen et al. (2002, 2003) their observations seem to contradict the predictions of the resonant transmission model ('sunspot filter theory', Settele et al. 1999, 2001, and references given there) mentioned in the Introduction: these observations show one dominant oscillation frequency while there are several power peaks almost equally spaced in frequency in the transmission curve calculated for the higher sunspot atmosphere. However, such a comparison has to consider the assumptions of the modelling: the theoretical transmission coefficient is valid for an incoming wave flux which is constant over all frequencies (a 'white flux'). Any other frequency structure in the wave flux incident from below—for example due to subphotospheric resonators—will modify the picture because the transmission coefficient has to be weighted with this frequency distribution to predict the oscillations at higher levels of the sunspot atmosphere (see drawing shown in Fig. 9).

5. Conclusions

The temporal occurrence of oscillations in intensity δI hints at deviations from an adiabatic behaviour which is assumed for most theoretical modelling (Tab. 3). Regions

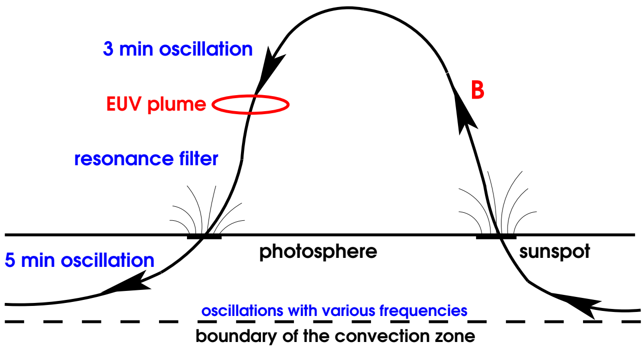

Fig. 9. Sketch showing the connection between oscillations of various frequencies emerging from the convection zone into the photosphere (with a dominating 5-min oscillation) passing a filtering region. In regions like bright EUV plumes above sunspots shorter period oscillations near 3 min become dominant.

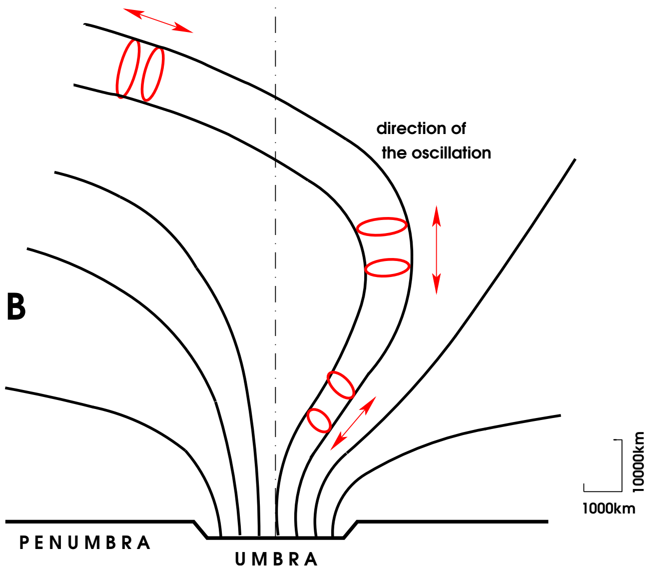

Fig. 10. Curved magnetic field lines above sunspots may be a reason for varying line-of-sight components of the Doppler velocity if an oscillating volume is moving along the field lines. (Scale vertically reduced by a factor of about 10.)

showing only velocity oscillations should be regarded as nearly adiabatic. The observed intensity oscillations imply that the CCTR can be considered to be almost isothermal at least for some periods of time.

Variations in the observable frequencies ('drift' indicated in Tab. 3) hint at highly non-stationary conditions in the CCTR. Models assuming a parallel stratification could explain the observed drift of the frequency of velocity oscillations towards higher frequencies through a shrinking size of the resonator. Such a geometrical situation is drawn in Fig. 10. The magnetic field in the vicinity of sunspots modifies the observability of oscillations and provides additional hints at downward moving oscillating elements in magnetic cylinders or cones existing in the CCTR and becoming observable for typical time scales of half an hour. Phase relations between the intensity and velocity data are probably as non-stationary as the oscillations themselves.

The sudden change in visibility or occurrence of the observed oscillations in EUV plumes above sunspots may indicate analogous processes to those observed in active region loops or other more dramatic events.

Acknowledgements. Axel Hofmann, AIP, kindly provided the extrapolation of the magnetic field. Part of this work was supported by the German *Deutsche Forschungsgemeinschaft, DFG* project number STA 351/4 and by the Federal Ministry of Education and Research through the German Space Agency DLR through grant No. 50 QL 9601 9. The SUMER project is financially supported by DLR, CNES, NASA and ESA PRODEX Programme (Swiss contribution). SUMER is part of SoHO, the Solar and Heliospheric Observatory, of ESA and NASA.

References

Bogdan, T.J. 2000, Sol. Phys., 192, 373
Brković, A., Rüedi, I., Solanki, S.K. et al. 2000, A&A, 353, 1083
Brynildsen, N., Leifsen, T., Kjeldseth-Moe, O. et al. 1999a, ApJ 511, L121
Brynildsen, N., Maltby, P., Leifsen, T., Kjeldseth-Moe, O., Wilhelm, K. 1999b, Sol. Phys. 191, 129
Brynildsen, N., Maltby, P., Fredvik, T., Kjeldseth-Moe, O., Wilhelm, K. 2001, Sol. Phys. 198, 89
Brynildsen, N., Maltby, P., Fredvik, T., Kjeldseth-Moe, O. 2002, Sol. Phys., 207, 259
Brynildsen, N., Maltby, P., Kjeldseth-Moe, O., Wilhelm, K. 2003, A&A, 398, L15
Curdt, W., Heinzel, P. 1998 ApJ, 503, L95
Curdt, W., Dwivedi, B.N., Feldman, U. 2000, JApA, 21, 397
DeMoortel, I., Ireland, J., Hood, A.W., Walsh, R.W. 2002, A&A, 387, L13
Fludra, A. 1999, A&A, 344, L75
Fludra, A. 2001, A&A, 368, 639
Gelfreikh, G.B., Grechnev, V., Kosugi, T., Shibasaki, K. 1999, Sol. Phys., 185, 177
Gurman, J.B., Leibacher, J.W., Shine, R.A., Woodgate B.E., Henze, W. 1982, ApJ, 253, 939
Harrison, R.A., Lang J., Brooks, D.H., Innes, D.E. 1999, A&A, 351, 1115
Henze, W., Tandberg-Hanssen, E., Reichmann, E.J., Athay, R.G. 1984, Sol. Phys., 91, 33
Hildebrandt, J., Staude, J. 2002, in: '1st Potsdam Thinkshop on Sunspots and Starspots', Poster Proc., ed. K.G. Strassmeier & A. Washuettl, 95
Ireland, J., Walsh R.W., Harrison, R.A., Priest, E.R. 1999 A&A, 347, 355
Maltby, P., Brynildsen, N., Fredvik, T., Kjeldseth-Moe, O., Wilhelm, K. 1999, Sol. Phys., 190, 437
O'Shea, E., Banerjee, D., Doyle, J.G., Fleck, B., Murtagh, F. 2001, A&A, 368, 1095
Rendtel, J. 2001, PhD thesis, Univ. Potsdam.
Settele, A., Zhugzhda, Y.D., Staude, J. 1999, Astron. Nachr., 320, 147
Settele, A., Zhugzhda, Y.D., Staude, J. 2001, Sol. Phys. 202, 281
Shibasaki, K. 2001, ApJ, 550, 1113

Staude, J., 1999, in: ASP Conf. Ser., Vol. 184, 'Magnetic Fields and Oscillations'. 3rd Adv. in Solar Physics Euroconf., ed. B. Schmieder, A. Hofmann & J. Staude (San Francisco: ASP), 113

Staude, J., Rendtel, J., Settele, A., 2001, in: 'Recent Insights into the Physics of the Sun and Heliosphere: Highlights from SOHO and Other Space Missions'. Proc. IAU Symp. 203, ed. P. Brekke, B. Fleck & J.B. Gurman. PASP, 320

Staude, J., Žugžda, Y.D., Locāns, V. 1985, Sol. Phys. 95, 37

Thomas, J.H., Cram, L.E., Nye A.H. 1984, ApJ, 285, 368

Wilhelm, K., Curdt, W., Marsch, E, et al. 1995, Sol. Phys., 162, 189

Torrence, C., Compo, G.P. 1998, Bull. Amer. Met. Soc., 79, 61

Žugžda, Y.D., Locāns, V., Staude, J. 1983, Sol. Phys., 82, 369

Žugžda, Y.D., Locāns, V., Staude, J. 1987, Astron. Nachr., 308, 257

Žugžda, Y.D., Staude, J., Locāns, V. 1984, Sol. Phys., 91, 219